

Impact of antibiotics on membrane vesicle production in Group B *Streptococcus*

Macy E. Pell,¹ Cole R. McCutcheon,¹ Jennifer A. Gaddy,^{2,3,4} David M. Aronoff,⁵ Margaret G. Petroff,^{1,6} Shannon D. Manning¹

AUTHOR AFFILIATIONS See affiliation list on p. 16.

ABSTRACT Group B *Streptococcus* (GBS) is an important bacterial pathogen during pregnancy, colonizing up to 35% of pregnant people recto-vaginally. Intrauterine GBS infection during pregnancy can cause preterm labor, early membrane rupture, and, if the fetus gets infected, stillbirth or early-onset disease (EOD) following birth. Intrapartum antibiotics are recommended to treat GBS-colonized pregnant patients during labor to prevent these outcomes, particularly EOD. However, persistent GBS colonization has been observed despite antibiotic treatment. One strategy employed by bacteria to promote survival and antibiotic tolerance is the production of membrane vesicles (MVs). To understand how GBS MVs are affected by antibiotics and influence bacterial survival, we exposed a clinical GBS strain recovered from a pregnant patient with persistent colonization to antibiotics and examined the impact on MV production and composition. Using nanoparticle tracking analysis, microscopy, and proteomics, antibiotic treatment of GBS was found to significantly increase the production of MVs relative to untreated GBS (control) regardless of the antibiotic class (ampicillin; $P = 4.2 \times 10^{-6}$, erythromycin; $P = 0.01$). Moreover, antibiotic exposure yielded MVs with different protein composition compared to the untreated control, with 21 and 19 proteins unique to the ampicillin- and erythromycin-treated GBS, respectively. Increased abundance of antibiotic-specific protein targets was observed in the respective antibiotic-treated MVs, suggesting a mechanism for evading antibiotic-mediated killing. Together, these data suggest that antibiotic treatment alters both the production and composition of MVs, which can promote GBS survival in such conditions.

IMPORTANCE GBS colonization during pregnancy can lead to invasive disease in neonates. Although antibiotics are given to GBS-positive pregnant patients during labor, some of these individuals remain colonized with GBS after treatment. Persistent GBS colonization is a public health concern, threatening the effectiveness of antibiotics and increasing the risk of GBS disease, especially for subsequent pregnancies. Although mechanisms linked to persistent colonization and antibiotic tolerance are poorly understood in GBS, MV production has been shown to promote bacterial survival in other species with and without antibiotic exposure. Herein, we demonstrated that two different antibiotics trigger changes in the production and composition of MVs in a persistent GBS colonizing strain, providing insight into the mechanisms used by GBS to rebound following antibiotic prophylaxis. Knowledge gained from this study can guide efforts in the development of more targeted and effective treatments for GBS disease.

KEYWORDS Group B *Streptococcus*, *Streptococcus agalactiae*, membrane vesicles, antibiotic use, proteomics

GBS is an opportunistic pathogen that causes disease in pregnant people and their neonates. While vaginal GBS colonization is typically asymptomatic, it can lead to preterm birth, stillbirth, or sepsis if transferred to the fetus or neonate (1). During the

Editor Fikri Y. Avci, Emory University School of Medicine, Atlanta, Georgia, USA

Address correspondence to Shannon D. Manning, manning71@msu.edu.

The authors declare no conflict of interest.

See the funding table on p. 16.

Received 9 December 2024

Accepted 29 April 2025

Published 9 June 2025

This is a work of the U.S. Government and is not subject to copyright protection in the United States. Foreign copyrights may apply.

late third trimester, rectovaginal GBS colonization affects 11%–35% of patients though variation has been reported by geographical region (2). Global estimates from 2015 indicate that 319,000 babies develop GBS infections each year (1).

Prevention of GBS disease involves screening for rectovaginal colonization at 36–37 weeks' gestation and administering intrapartum antibiotic prophylaxis (IAP) to GBS-positive patients (3). β -Lactam antibiotics like penicillin and ampicillin are recommended for IAP, but macrolides are recommended for patients reporting severe penicillin allergies (3). IAP has successfully reduced rates of neonatal early onset disease (EOD), which presents as bacteremia, pneumonia, or meningitis within the week following birth (4, 5). However, IAP has not reduced rates of preterm births, stillbirths, or late onset disease (LOD), which results in bacteremia or meningitis 1 week to 3 months after birth (4, 5). Increasing frequencies of clindamycin- and erythromycin-resistant GBS have been reported (6) as well as persistent vaginal colonization for up to 6 weeks postpartum despite antibiotic treatment (7), which both threaten the effectiveness of IAP.

The polysaccharide capsule is critical for virulence (8) and is used to classify GBS into 1 of 10 (Ia, Ib, II-IX) capsule (cps) types (serotypes). Strains with cps type III account for 61.5% of invasive GBS disease cases worldwide (9). Additional classification methods, such as multilocus sequence typing (MLST), have led to the discovery of a hypervirulent lineage, sequence type (ST)–17, which mostly comprises cps III strains and predominates among neonatal disease cases relative to other STs (10–12). Hypervirulence is partly due to their enhanced ability to adhere to and invade host cells, resist phagosomal stress, and escape antibiotic-mediated killing (13, 14). Furthermore, ST-17 strains were more likely to persist in patients with vaginal colonization after IAP and childbirth (15, 16), demonstrating their resiliency even in the presence of antibiotics.

To evade common stressors, many Gram-negative and -positive bacteria release membrane vesicles (MVs) that contain multiple components including toxins, virulence factors, nucleic acids, lipoproteins, and enzymes (17, 18). These MVs are biologically active and have been shown to upregulate pro-inflammatory immune responses and initiate the disease process in the absence of live bacterial cells (18). We and others have described the production of MVs in GBS (19–22), demonstrating that they contain virulence components involved in attaching to and invading host cells, reducing oxidative killing, and eliciting pro-inflammatory host responses. We further demonstrated that MVs varied across STs; MVs from a ST-17 strain had a higher concentration of virulence factors (20).

Prior studies of *Pseudomonas aeruginosa*, *Escherichia coli*, and *Staphylococcus aureus* have shown that antibiotics enhance the production of MVs (23–28). Moreover, MVs secreted by methicillin-resistant *S. aureus* after β -lactam antibiotic exposure contained proteins linked to antibiotic degradation (29), a result that was also observed in *E. coli* (28). These findings along with the identification of MVs within biofilms in *P. aeruginosa* (30) highlight their potential impact on bacterial adaptation and survival during antibiotic stress. No studies, however, have been conducted in GBS to determine how exposure to antibiotics that are routinely used for IAP can impact MV production. Our findings demonstrate that antibiotics induce MV biogenesis and alter their protein composition, highlighting a potential role for MVs in adaptation and survival during antibiotic stress.

MATERIALS AND METHODS

Bacterial growth conditions

The postpartum GBS isolate, GB00112 (31) was used for all experiments following culture in Todd-Hewitt broth (THB) or on Todd-Hewitt agar (THA) (BD Diagnostics, Franklin Lakes, New Jersey, USA) and an overnight incubation at 37°C with 5% CO₂. Colony-forming units (CFUs) were quantified by serially diluting samples in 1× phosphate-buffered saline (PBS) and plating on THA with an Eddy Jet spiral plater (IUL Instruments, Barcelona, Spain) in logarithmic mode. CFUs were enumerated from plate images in Microsoft

PowerPoint v16.66.1 using the spiral plater counting grid overlay. The absorbance or optical density (OD₆₀₀) and CFUs were measured every hour for a total of 8 and 6 h, respectively, for GB00112 grown with and without ampicillin (2.5 µg/mL) or erythromycin (10 µg/mL); assays were performed in triplicate.

Membrane vesicle isolation and purification

Isolation of MVs was performed as described (20) with some modifications. Briefly, overnight cultures of GB00112 were back diluted 1:50 and grown to early/mid-log phase (OD₆₀₀ 0.35–0.45). Following centrifugation at 2,000 × *g* for 10 min, the cells were resuspended in 100 mL of fresh THB with ampicillin, erythromycin, or no antibiotics (untreated control) and incubated for 4 h. Next, the cultures were centrifuged at 2,000 × *g* for 20 min at 10°C to pellet bacterial cells. The supernatant was subjected to further centrifugation, filtration, and concentration followed by ultracentrifugation to pellet the MVs. Each pellet was resuspended in a final volume of 100 µL of 1× PBS and stored at –80°C until use.

To isolate the MVs, the Problock Gold Bacterial Protease Inhibitor Cocktail (GoldBio, St. Louis, MO, USA) was added to the concentrated supernatants to prevent protein degradation. Following ultracentrifugation, resuspended samples were purified using qEV1 size exclusion columns (IZON Science, Christchurch, New Zealand) according to the manufacturer's instructions. The qEV1 size exclusion columns have a minimum cutoff size of 35 nm, which is appropriate to capture GBS MVs that were found to be no less than 40 nm in crude MV preparations from GBS grown in normal culture conditions without antibiotics (20). These columns were chosen to ensure capture of bacterial MVs rather than other fragments or particles found within the supernatant, which could result in an overestimate of MV production. The resulting fractions were further concentrated using Amicon Ultra-4 (10 kDa cutoff) centrifugal filters (Millipore Sigma) to a final volume of ~100–200 µL. More protease inhibitor was added to the concentrated MV fractions, which were also stored at –80°C.

Electron microscopy of bacterial cells and membrane vesicles

Scanning electron microscopy (SEM) was performed on bacterial samples collected after the 4 h antibiotic treatment and prepared as described in our prior study (20) with some modifications. All resting and washing times were performed for 10 min, and samples were coated with osmium of ~5 nm thickness. Samples were imaged using a JEOL 7500F scanning electron microscope (JEOL Ltd., Tokyo, Japan).

Bacterial cells were also visualized by thin-section transmission electron microscopy (TEM). Samples were collected after the 4 h antibiotic treatment, pelleted, and fixed with 2.5% glutaraldehyde solution in phosphate-buffered saline (PBS). Samples were then washed with 0.1 M phosphate buffer, postfixed with 1% osmium tetroxide in 0.1 M phosphate buffer, dehydrated in a gradient series of acetone, and infiltrated and embedded in Spurr. A Power Tome Ultramicrotome (RMC, Boeckeler Instruments, Tucson, AZ) was used to obtain 70 nm thin sections that were post stained with uranyl acetate and lead citrate. TEM was also performed on the MVs to confirm purity; 5 µL samples from each treatment were fixed with 2.5% glutaraldehyde in PBS and prepped as described (20). Both MV and thin-sectioned bacterial samples were imaged using a JEOL 1400 Flash Transmission Electron Microscope (Japan Electron Optics Laboratory, Japan) at an accelerating voltage of 100 kV.

Membrane vesicle quantification

Isolated MVs were quantified via nanoparticle tracking analysis using a NanoSight NS300 (Malvern Panalytical, Westborough, MA, USA) as described previously (20) to make comparisons across treatment groups (*n* = 6 replicates). Samples were diluted in PBS (1: 1,000–1:10,000) for each replicate, and the data were averaged across five technical replicates of nanoparticle tracking videos per biological replicate for each treatment

group. Raw output was exported as a .csv file and analyzed in R v4.1.2 (<https://www.r-project.org/>) using the tidyNano package (32). MV counts were normalized to the total culture volume used for preparation and the final volume used for resuspension. Values outside of the interquartile range $\times 1.5$ were deemed outliers.

Membrane vesicle proteomics

Purified MV fractions ($n = 4$ biological replicates per treatment) were subjected to liquid chromatography-tandem mass spectrometry (LC-MS/MS), and protein concentrations were quantified using the Pierce Bicinchoninic Acid (BCA) Assay (Thermo Fisher Scientific, Waltham, MA, USA) following the microplate procedure with 10 μL sample volumes according to the manufacturer's instructions. Fractions were supplemented with 2% SDS in water to reduce excess background signal from lipids, and 0.5 μg of MV protein for each sample was loaded into 4-20% Tris-Glycine SDS-PAGE gels (BioRad, Hercules, CA, USA) and concentrated into single bands that were fixed, stained, and excised as described (20).

For proteolytic digestion, gel bands were digested in-gel as we described in our prior study with minor modifications (20). For LC-MS/MS, an injection of 5 μL was automatically made using a Thermo EASYnLC 1000 onto a Thermo Acclaim PepMap RSLC 0.1 mm \times 20 mm C18 trapping column and washed for ~ 5 min with buffer A. Bound peptides were eluted over 35 min onto a Thermo Acclaim PepMap RSLC 0.075 mm \times 250 mm resolving column with a gradient of 5%B to 40%B in 24 min, ramping to 90%B at 25 min and held at 90%B for the duration of the run (Buffer A = 99.9% Water/0.1% Formic Acid, Buffer B = 80% Acetonitrile/0.1% Formic Acid/19.9% Water) at a constant flow rate of 300 nL/min. Column temperature was kept constant at 50°C using an integrated column oven (PRSO-V1, Sonation GmbH, Biberach, Germany), and eluted peptides were sprayed into a ThermoScientific Q-Exactive mass spectrometer using a FlexSpray spray ion source. Survey scans were taken in the Orbi trap (35,000 resolution, determined at m/z 200), and the top 15 in each scan was subjected to automatic higher energy collision-induced dissociation (HCD) with fragment spectra acquired at 17,500 resolution.

The resulting MS/MS spectra were converted to peak lists using Mascot Distiller, v2.8.2, and searched against a protein database containing all sequences available for *S. agalactiae*. These sequences were downloaded from Uniprot (<https://www.uniprot.org/>) and appended with common laboratory contaminants (<https://www.thegpm.org/>, cRAP project) using the Mascot searching algorithm v2.8.0.1 (33). Mascot output was analyzed with Scaffold, v5.1.2 to validate protein identifications; assignments with a 1% false discovery rate (FDR) confidence filter were considered true. Mascot parameters were as follows; allow up to two missed tryptic sites, fixed modification of Carbamido-methyl Cysteine, variable modification of Oxidation of Methionine, peptide tolerance of ± 10 ppm, MS/MS tolerance of 0.02 Da, and FDR calculated using randomized database search.

Data analysis

All raw data were wrangled, visualized, and analyzed using R v4.1.2 (<https://www.r-project.org/>) in RStudio. Specifically, data wrangling was performed using devtools v2.4.5 (<https://devtools.r-lib.org/>) as well as dplyr v1.1.3 (<https://dplyr.tidyverse.org/>), purr v1.0.2 (<https://purrr.tidyverse.org/>), readr v2.1.4 (<https://readr.tidyverse.org/>), and tidyr v1.3.0 (<https://tidyr.tidyverse.org/>) through tidyverse (34). Data were visualized using EnhancedVolcano v1.13.2 (doi: 10.18129/B9.bioc.EnhancedVolcano), ggplot2 (35), ggbeeswarm v0.7.2 (<https://cran.r-project.org/package=ggbeeswarm>), VennDiagram v1.7.3 (36), and viridis v0.6.4 (<https://cran.r-project.org/web/packages/viridis/vignettes/intro-to-viridis.html>) packages. For proteomics, total spectrum counts were exported from spectrum identification files via Scaffold v5.1.2 with the following filters: 95% protein threshold, 1.0% FDR peptide threshold, and a minimum of 2 peptides.

To test for normality, Shapiro-Wilk tests were performed using the R stats package. For non-normally distributed data, Kruskal-Wallis and Dunn's tests were used with the

asbio v1.9-6 (<https://rdrr.io/cran/asbio/>) and rstatix v0.7.2 (37) packages, respectively. The one-way ANOVA and Tukey's Highly Significant Difference (HSD) test were applied to normally distributed data using rstatix. Comparisons were made between each treatment group relative to the control group separately at a given time point to detect differences in bacterial growth (OD_{600}), bacterial quantity (CFUs/mL), and MV protein abundance (spectral counts). Vegan v2.6-4 (<https://cran.r-project.org/web/packages/vegan/>) was used for the Principal Coordinates Analysis (PCoA) using Euclidean distance metrics on MV protein spectral counts. A permutational multivariate analysis of variance (PERMANOVA) test with 999 permutations was performed on the resulting PCoA distance matrix using `vegan::adonis2` and `pairwiseAdonis` v0.4.1 (<https://github.com/pmartinezarbizu/pairwiseAdonis>). *P*-values < 0.05 were considered significant.

RESULTS

Viable cells exist after antibiotics

Since IAP guidelines recommend antibiotic administration for a minimum of 4 h before birth (3), we quantified growth of GBS strain GB00112 following exposure to 10× the minimum inhibitory concentration of ampicillin and erythromycin. GB00112 was sequenced previously (31) and is susceptible to both antibiotics (7). The OD_{600} and CFUs were measured hourly for 8 and 6 h, respectively. Ampicillin treatment rapidly reduced absorbance 1-h post-treatment, while erythromycin treatment had a delayed growth reduction (Fig. 1A). Similarly, a significant reduction in CFUs was observed for both treatments when each was compared to the control group at 1 h (Fig. 1B).

SEM of the GBS cultures detected intact cells along with the presence of extracellular particles in all samples regardless of treatment (Fig. S1). The ampicillin-treated cultures had more extracellular particles compared to the control and erythromycin-treated cultures. Based on the identification of MVs produced by the same strain in our prior study when grown in THB without antibiotics (20), we hypothesized that these abundant extracellular particles are also MVs.

MV production increases during antibiotic stress

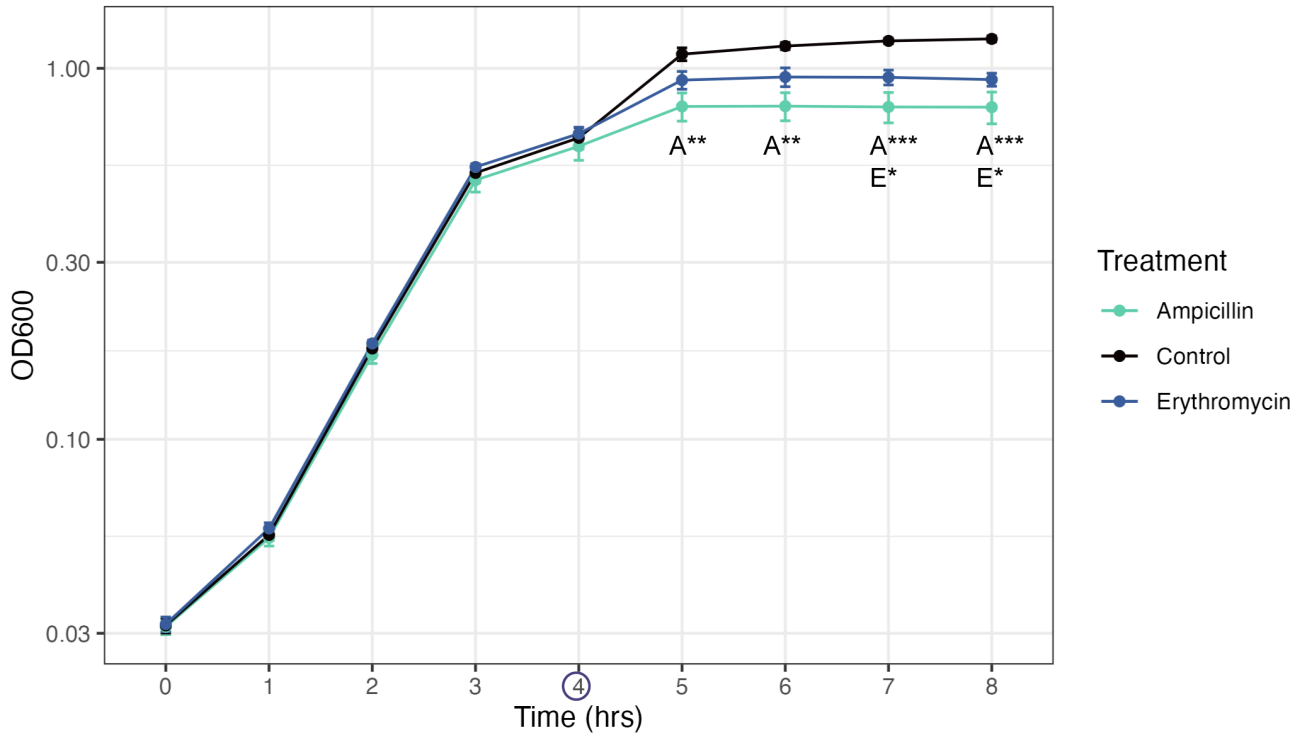
To confirm that the extracellular particles were MVs, a previously established protocol was used to isolate MVs from antibiotic-treated GBS (20). Use of TEM detected MVs, which are shown by the presence of dark, electron-dense circles enclosed by a bright membrane of ~100–150 nm, in all cultures regardless of treatment (Fig. 2).

Next, we sought to quantify the abundance of MVs produced with and without antibiotics. Use of nanoparticle tracking analysis uncovered three highly similar MV sizes (nm) with variable average particle counts in each treatment group (Fig. 3A). The most abundant sizes measured 122.5 nm, 127.5 nm, and 118.5 nm, for the ampicillin-treated, erythromycin-treated, and control groups, respectively. Plotting the percentage of the total particles by particle size (nm) further confirmed a slight difference in size per treatment group (Fig. S2). Importantly, the total number of MVs differed significantly between the three treatment groups (Fig. 3B). When compared to the untreated control cultures, which had an average of 4.6×10^9 MVs per sample, the ampicillin-treated cultures had an average of 3.5×10^{10} MVs per sample (Tukey's HSD test $P = 4.2 \times 10^{-6}$). The erythromycin-treated cultures had an average of 1.5×10^{10} MVs per sample, which also differed from the control cultures (Tukey's HSD test $P = 0.01$). In addition, the number of MVs in the ampicillin-treated cultures was significantly greater than the number recovered from the erythromycin-treated cultures (Tukey's HSD test $P = 0.002$).

Distressed membranes provide insight into the mechanism of excess MV production

Since enhanced MV production was observed with both antibiotic treatments, thin-section TEM was used to visualize the effect of each antibiotic on bacterial cell integrity and to ensure that the cells were still viable despite treatment. In all treatment groups,

A.



B.

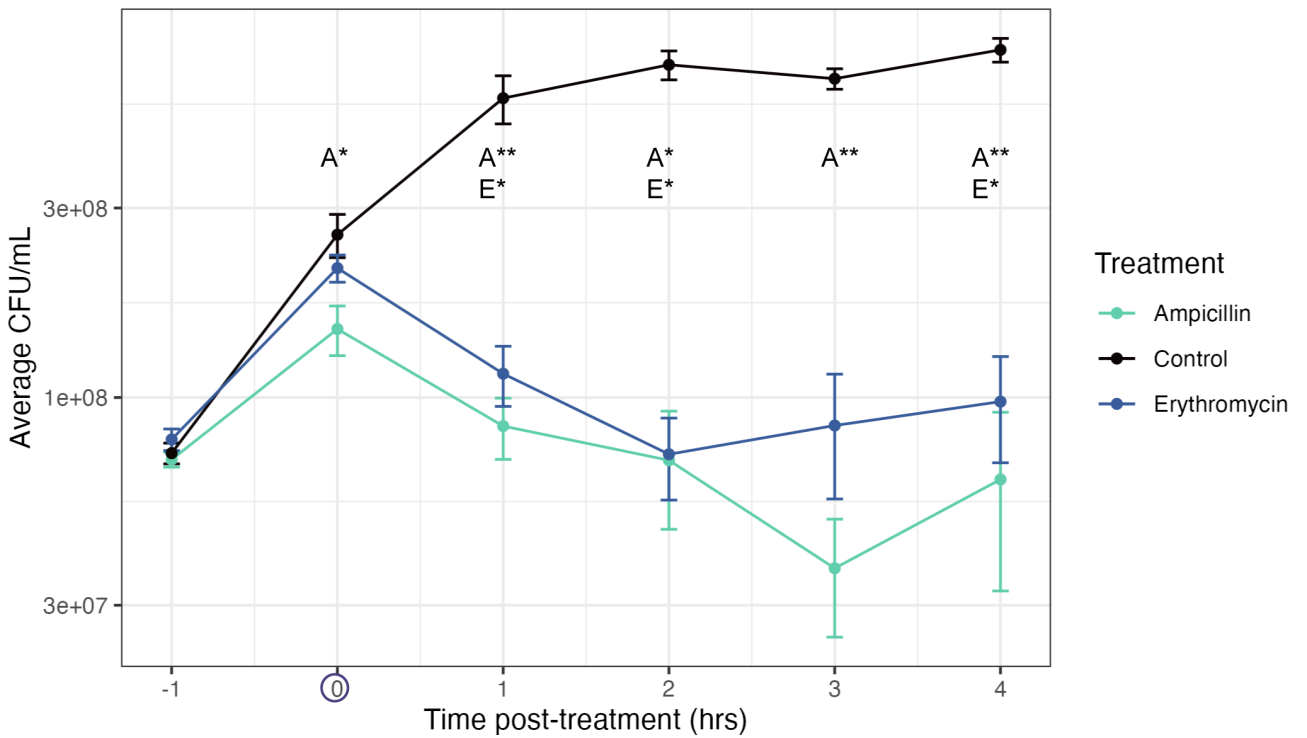


FIG 1 Antibiotics impact GBS growth. The average (A) absorbance (OD₆₀₀) and (B) viable colony-forming units (CFUs)/mL following treatment with ampicillin (turquoise) or erythromycin (blue) is shown relative to untreated cells (control; black). Error bars reflect standard error for each timepoint ($n = 4$ biological replicates). (Continued on next page)

Fig 1 (Continued)

replicates). Antibiotics were added to cultures after 4 h of growth, which represented as time point 0 (circled on the x-axis). (A) OD_{600} measurements (y-axis) were taken every hour for 8 h (x-axis), whereas (B) CFUs were determined 1 h before the treatment period (−1). The data at the following time points were not normally distributed: 3, 4 (OD_{600}), 5, 6, 7, and 8 (CFU/mL). For non-normally distributed data, the Kruskal-Wallis and Dunn's tests were used to test for differences in the mean of each treatment group ("A" = ampicillin, "E" = erythromycin) relative to the mean of the control group separately at each time point. The data from the remaining time points were normally distributed, and thus, a one-way ANOVA and Tukey's HSD test were applied. The treatments (A or E) with significant differences are indicated in the figure and P -values <0.05 , <0.01 and <0.001 are noted by *, **, and ***, respectively.

the images show dark, electron-dense viable cells (Fig. 4; Fig. S3). Non-viable cells were also detected in each treatment group though the antibiotic-treated cultures had less electron dense cells throughout and more empty "ghost" cells. Ghost cells were previously described in *S. aureus* upon exposure to quinupristin/dalfopristin (38). In the untreated cultures, most of the bacterial cells were surrounded by an intact and distinct membrane and had a visible septum structure in the dividing bacteria. By contrast, the ampicillin-treated cells had a less-distinct cell membrane with a distressed appearance. Areas of potential MV formation appear as blebs on the cell surface; these blebs were absent in the untreated cells but were observed in the ampicillin-treated cells. Although the erythromycin-treated cells had a more distinct and intact membrane than the ampicillin-treated cells, they still differed in appearance relative to the untreated cells. Cells exposed to erythromycin appear to have large membrane gaps and a thickened cell wall, which was demonstrated previously in *S. aureus* and may be indicative of defective cell division due to disruptions in protein synthesis (39).

MV protein composition differs by treatment

The protein composition of GBS MVs was evaluated using LC-MS/MS; 417 distinct proteins were identified among all MVs. The MVs from the untreated GBS had the most proteins ($n = 330$), followed by those from the erythromycin- ($n = 319$) and ampicillin-treated ($n = 276$) cells (Fig. 5A). Nearly half of the proteins ($n = 201$, 48.2%) were shared among all MVs, and 47 were shared between the antibiotic-treated MVs. Twenty-one proteins were unique to the MVs from ampicillin-treated GBS, whereas 19 were unique to the erythromycin-treated MVs and 70 were unique to the untreated MVs. Data reduction and visualization by PCoA using Euclidean distance revealed clustering of MV proteomes by treatment group (PERMANOVA $P = 0.001$; Fig. 5B). There was significant dissimilarity ($P = 0.001$) across samples and differences in

protein composition for ampicillin-treated vs control MVs ($P = 0.031$), erythromycin-treated vs control MVs ($P = 0.033$), and ampicillin- vs erythromycin-treated MVs ($P = 0.029$).

Among the 47 proteins unique to the antibiotic-treated MVs (Table S1), several are well-known virulence proteins like CylA, which is needed for hemolysin production. Hyaluronate lyase, an immune modulation factor, and DltS, an environmental sensor, were also detected. Other notable proteins shared between the antibiotic-treated MVs include transport proteins ($n = 10$), cell division proteins ($n = 4$), ribosomal proteins ($n = 4$), transferases ($n = 5$), membrane proteins ($n = 3$), and polysaccharide biosynthesis proteins ($n = 2$).

The 21 proteins unique to MVs recovered from the ampicillin-treated cultures included key virulence and stress proteins such as an antitoxin protein, a Gls24 protein, and a universal stress protein (Table S2). Comparatively, unique proteins detected in the MVs from erythromycin-treated cultures included virulence and stress-associated proteins such as the toxic anion resistance protein, alkaline shock protein, and the signal recognition particle receptor (FtsY). An even larger number of proteins were unique to the MVs from the untreated (control) cells and include those that are important for normal cell function such as GTPases, tRNA ligases, and DNA topoisomerases.

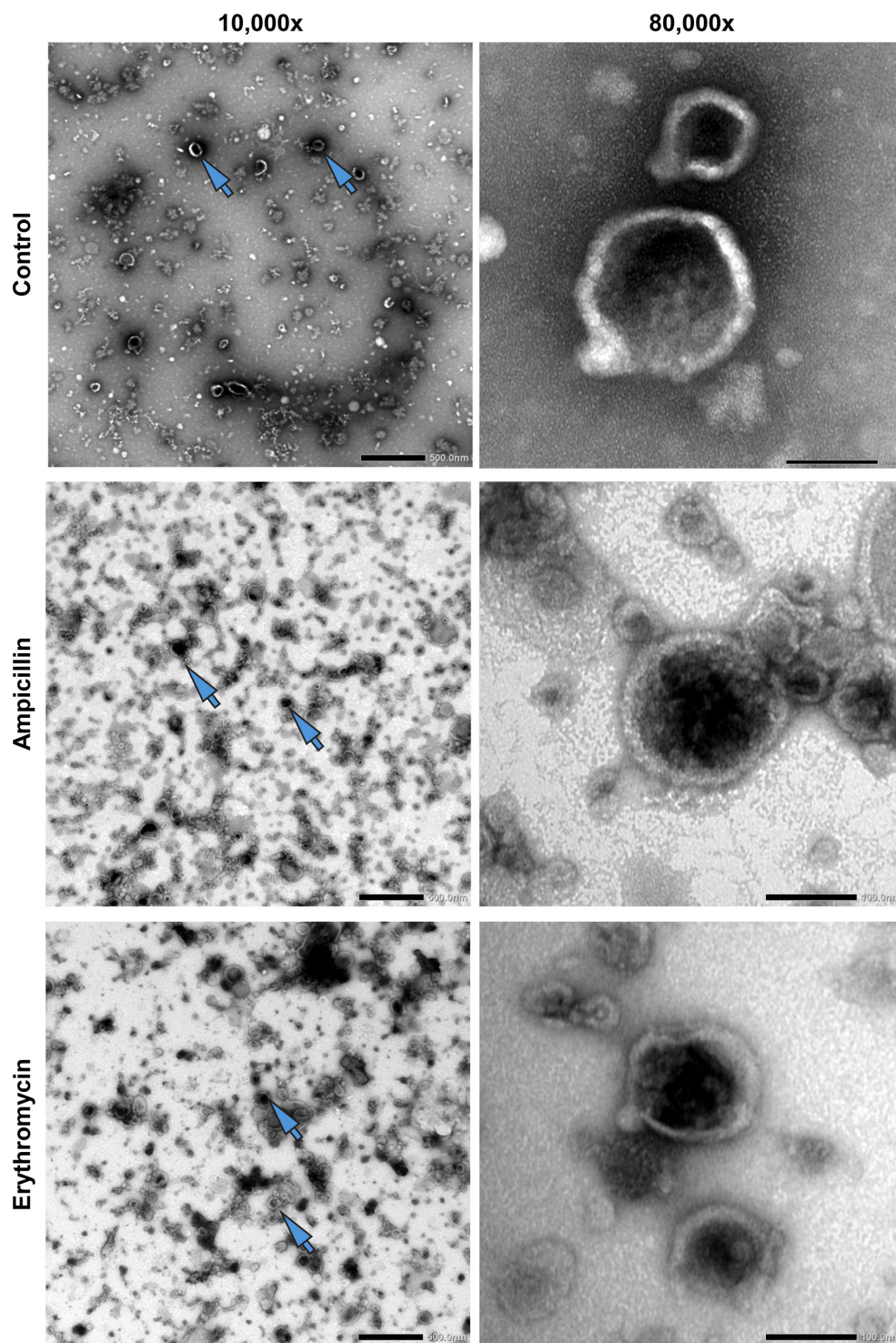


FIG 2 TEM shows the presence of MVs. MVs were isolated from GBS cultures grown without antibiotics (control, top) and after 4 h treatment with ampicillin (middle) or erythromycin (bottom). Scale bars represent 500 nm and 100 nm for 10,000 \times (left) and 80,000 \times (right) magnifications, respectively. MVs are identified by their spherical shape with a dark, electron-dense center surrounded by a bright membrane. Blue arrows point to representative MVs.

Shared MV proteins were differentially enriched across treatment groups

To compare the abundance of proteins packaged within the MVs, pairwise comparisons were performed using the average spectral counts of proteins shared between the

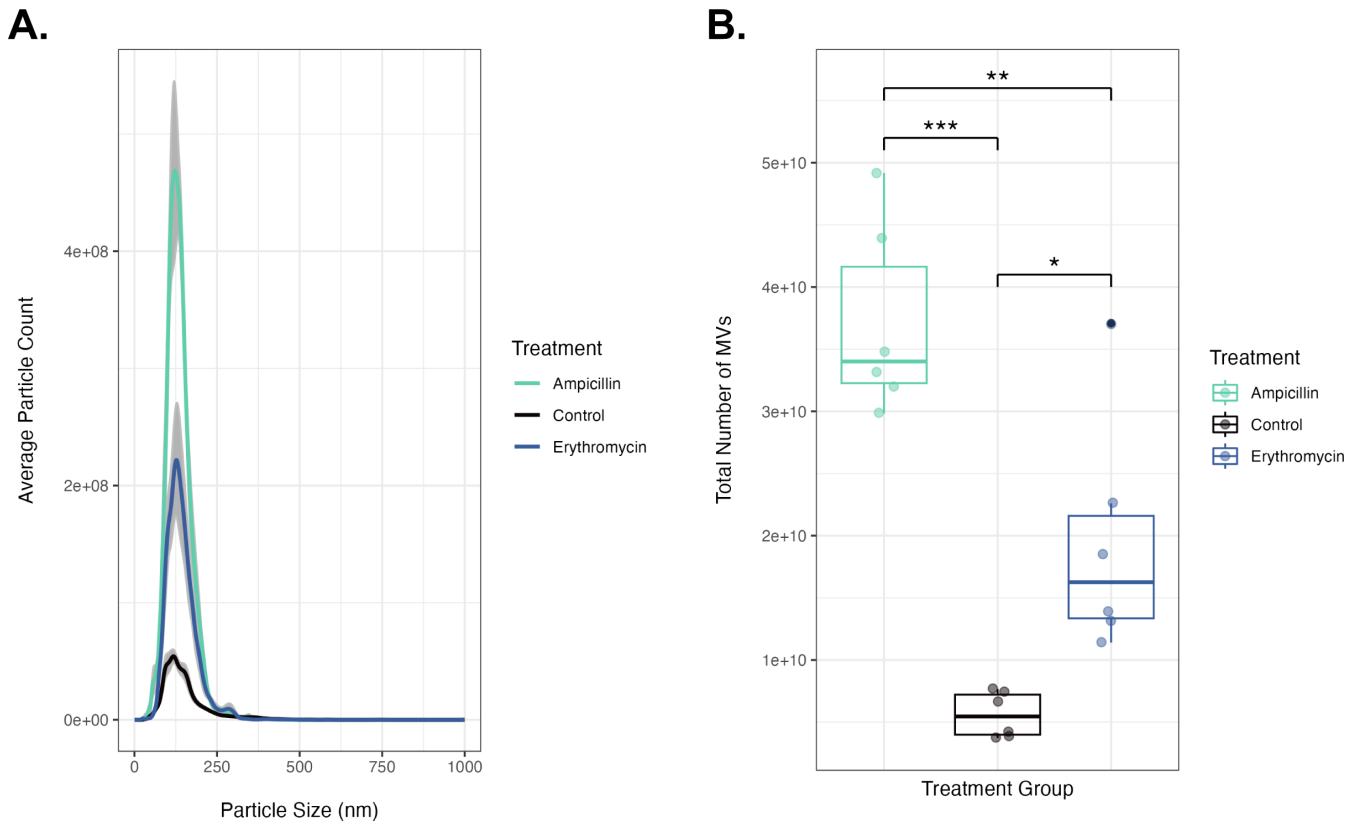


FIG 3 Number of MVs from GBS cultures with and without antibiotics. **(A)** Distribution of MV sizes (x-axis) in nanometers (nm) by average number of MVs ($n = 6$ replicates) from cultures treated with ampicillin (turquoise), erythromycin (blue), or without antibiotics (control, black). Gray shading is the standard error across replicates. **(B)** Boxplots show the total number of MVs (y-axis) per treatment group (x-axis) with dots for each biological replicate ($n = 6$); outlier replicates are shown as opaque black dots. One-way ANOVA and Tukey HSD tests examined differences between each antibiotic treatment relative to the control group or each other. P -values < 0.05 (*), < 0.01 (**), and < 0.001 (***) are shown.

ampicillin-treated and control MVs ($n = 208$), erythromycin-treated and control MVs ($n = 253$), or both antibiotic-treated MVs ($n = 248$). Significant differences in protein abundance, defined as a > 1.5 \log_2 -fold-change (FC) with a P -value < 0.05 , were observed for 50 proteins (Table S3).

Ampicillin induced the most robust alterations in MV protein composition with 22 differentially enriched proteins relative to the untreated control (Fig. 6A). These proteins included virulence factors, such as the serine protease, capsule (CpsD), stress response protein Gls24, an endolytic murein transglycosylase, and penicillin-binding proteins (Pbp2A, Pbp2B, and Pbp2X) that were detected in all three treatment groups. Other proteins including transport, cell division, and regulatory proteins were also more abundant in the ampicillin-treated MVs relative to the control MVs. By contrast, MVs from the erythromycin-treated cells had 10 differentially expressed proteins as compared to the control; these proteins included the chaperone protein DnaK, a stress response protein, and the 50S ribosomal subunit RplF (Fig. 6B).

Among the shared MV proteins from the cells treated with both antibiotics, 19 were differentially enriched among the ampicillin- and erythromycin-treated groups (Fig. 6C), demonstrating the distinct effects that these antibiotics have on MV composition. Most proteins were more abundant in the MVs produced by the erythromycin-treated cells, including a cell-wall associated protein (PcsB) and 10 ribosomal proteins (Fig. S4). The remaining seven proteins were more abundant in the MVs from the ampicillin-treated cells and were also linked to virulence. These included CAMP factor, cell wall integrity proteins (e.g., LytR-cpsA-psr [LCP] domain-containing protein), and penicillin-binding protein (PBP) 1B.

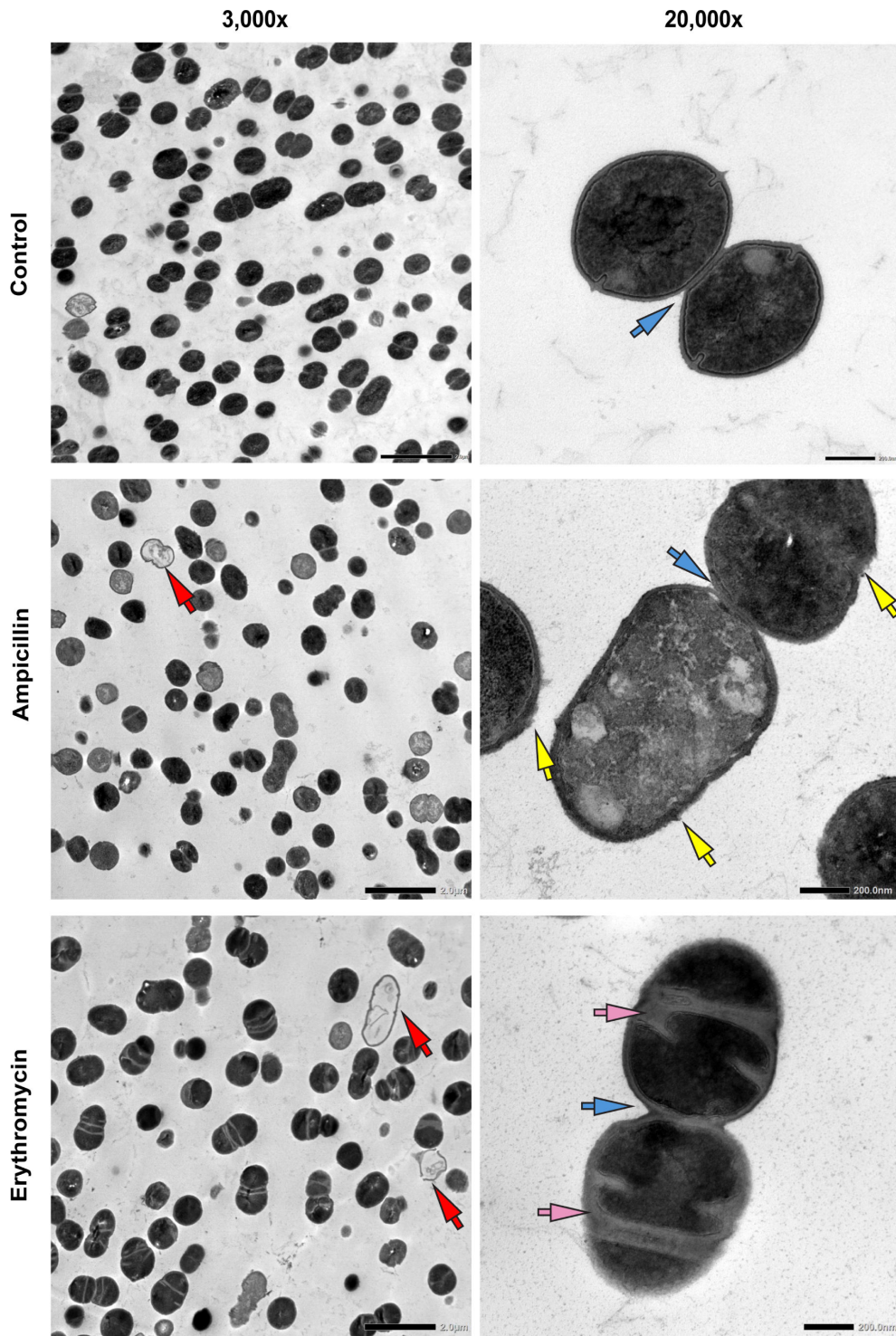


FIG 4 Thin section TEM images of GBS in the presence and absence of antibiotic treatment. GBS cultures were treated with erythromycin (bottom) and ampicillin (middle) for comparison to untreated cultures without an antibiotic (control, top). Scale bars represent 2.0 μ m and 200 nm for 3,000 \times (left) and 20,000 \times (right) magnifications, respectively. The red arrows show the non-viable “ghost cells,” the blue arrows show septa, pink arrows show thickened cell walls, and yellow arrows point to areas showing non-intact or distressed membranes and potential “blebs.”

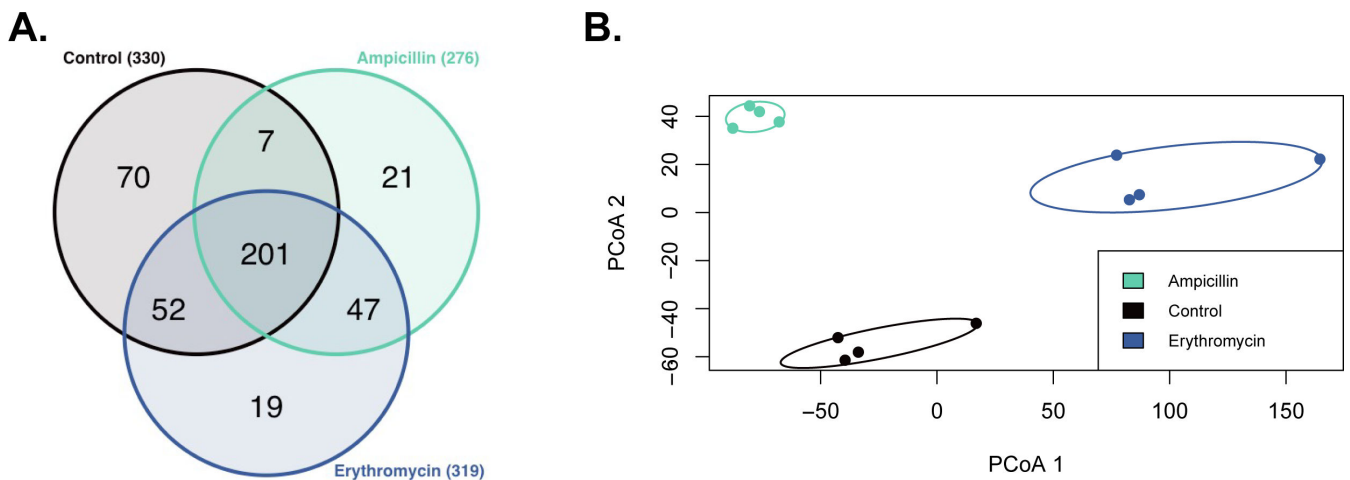


FIG 5 Distinct proteins are found in MVs from each treatment group. (A) Venn diagram showing the distribution of 417 distinct proteins detected among MVs from ampicillin- (turquoise) and erythromycin-treated (blue) cells as well as untreated control cells (black). The number of proteins identified in MVs from each treatment group is shown in parentheses, whereas the numbers within the Venn diagram highlight the shared proteins as well as those that are unique to each group. (B) A principal coordinate analysis (PCoA) with Euclidean distance shows the dissimilarities in MV protein content across ampicillin (turquoise), control (black), and erythromycin (blue) treatment groups. Individual points represent biological replicates ($n = 4$), while ellipses represent 95% confidence intervals of clustering. Points that are closer together are more similar.

Increased abundance of antibiotic-specific targets highlights a protective role of MVs

Penicillin-binding proteins (PBPs) are not only important for peptidoglycan synthesis but are also the main targets for β -lactam antibiotics. In addition to the four PBPs that were significantly more abundant in the ampicillin-treated MVs (Fig. 7A), PBP1A and FibA, a β -lactam resistance factor, were also highly abundant in MVs recovered from all three treatment groups. Of note, a sixth penicillin-binding protein, PBP4, was detected in MVs from both

antibiotic-treated groups, but not in the control MVs. Increased abundance of these PBPs along with the presence of notable cell-wall associated proteins demonstrates the protective potential of MVs against cell-wall targeting antibiotics, like ampicillin.

In contrast, erythromycin acts to inhibit protein synthesis by targeting the 50S ribosomal subunit. Although 22 50S ribosomal-related proteins were identified in MVs from all sample groups, two of these proteins, RplX and RpmL, were exclusive to the erythromycin-treated MVs. Of those that were identified in MVs from all three treatment groups ($n = 12$), five were significantly more abundant in erythromycin MVs relative to the control and/or ampicillin MVs (Fig. 7B). The abundance of 50S ribosomal proteins in the MVs from erythromycin-treated cells indicates a protective function of MVs against antibiotics like the macrolides, which inhibit protein translation.

DISCUSSION

Prior studies of GBS MVs isolated following growth in standard broth conditions have highlighted their role in inducing inflammation and reducing oxidative killing while promoting preterm birth and neonatal death *in vivo* (19, 21). Studies in other bacterial pathogens also have demonstrated that antibiotic treatment exacerbates MV production (23–28), which may promote antibiotic tolerance (28, 30). Through the experiments presented herein, we have demonstrated that exposure to two antibiotics commonly used for GBS IAP affects the quantity and protein composition of MVs produced by GBS, thereby impacting virulence and protection from antibiotic-mediated killing.

The significant increase in MV production observed in both ampicillin- and erythromycin-treated cultures relative to the untreated control suggests that antibiotic stress,

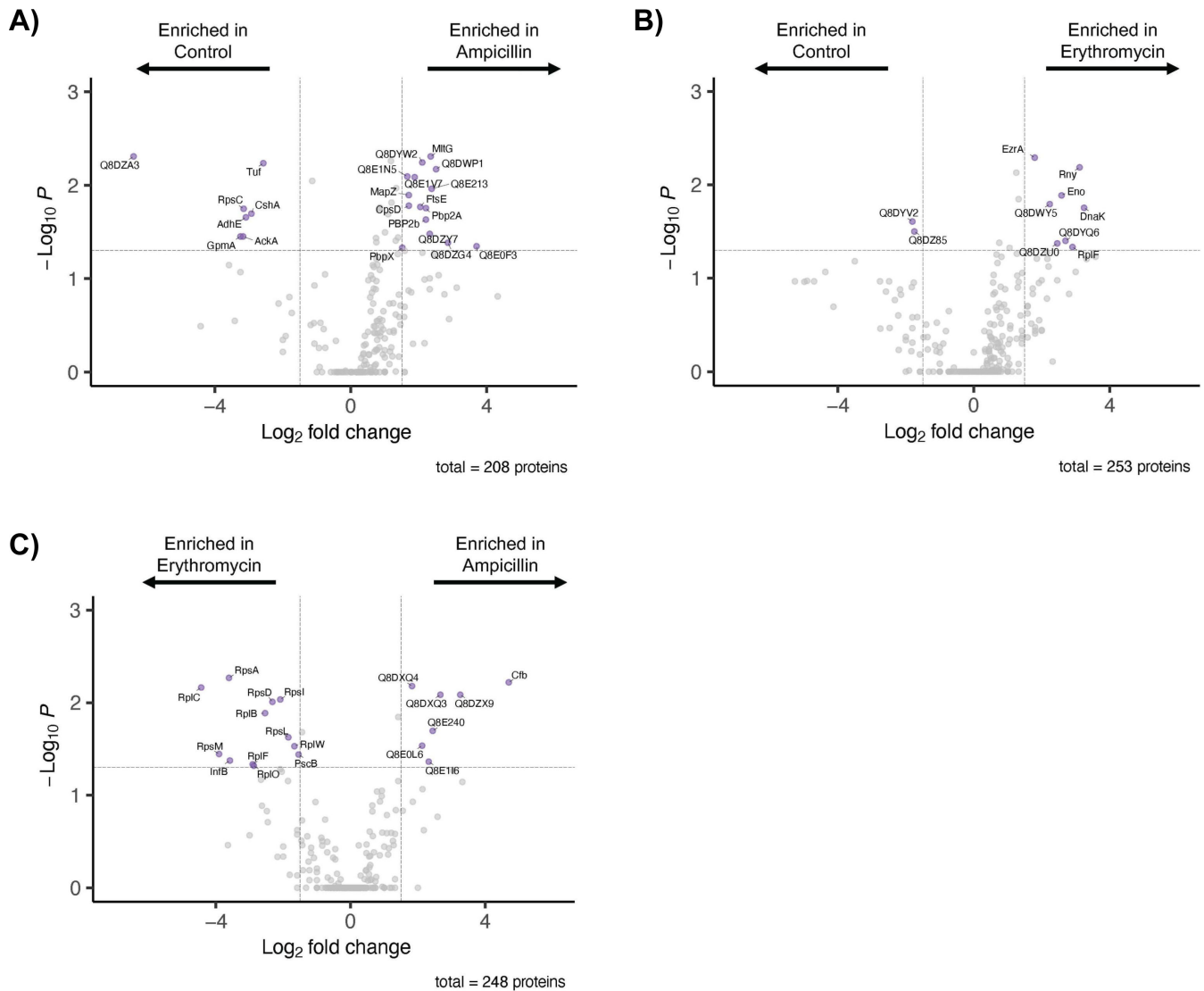


FIG 6 Differentially abundant MV proteins across treatment groups. Volcano plots show the differential abundance of proteins shared between (A) ampicillin and control MVs, (B) erythromycin and control MVs, and (C) ampicillin and erythromycin MVs. Pairwise Kruskal-Wallis tests assessed differences in protein abundance with P -values shown on the y -axis ($-\text{Log}_{10} P$ scale); a P -value < 0.05 was significant. Log_2 fold change values of mean spectral counts (x -axis) are shown relative to the first treatment group listed. For example, the fold change for the “Ampicillin vs. Control” (A) group was relative to the mean spectral counts of ampicillin MVs such that a Log_2 -fold-change > 1 represents proteins that are upregulated in ampicillin-treated cultures. A log_2 fold change cutoff of ± 1.5 (vertical dashed lines) and P -values < 0.05 (horizontal dashed line) identified differentially abundant proteins (purple, with ID labels).

regardless of the antibiotic type, affects MV production in GBS. Although other studies in both Gram-positive and Gram-negative species have reported increases in MV production during antibiotic exposure (23–28), the exact mechanisms that drive MV biogenesis in the presence of specific antibiotics are unclear. It has been suggested that increased production is due to weakening and/or lysis of the bacterial cell wall, DNA damage, and/or a general response to stress (40).

Since the strain (GB00112) used in our experiments is susceptible to both ampicillin and erythromycin (7), cell death may partly contribute to the significant increase in MV production observed following antibiotic exposure. Indeed, a significant reduction in bacterial growth and viable CFUs was observed in cells treated with both antibiotics relative to the untreated (control) cells. Although MV production requires metabolically active bacterial cells (41), weakening and lysis of the cell wall is thought to be a mechanism of MV release in Gram-positive species with a thick peptidoglycan layer (18).

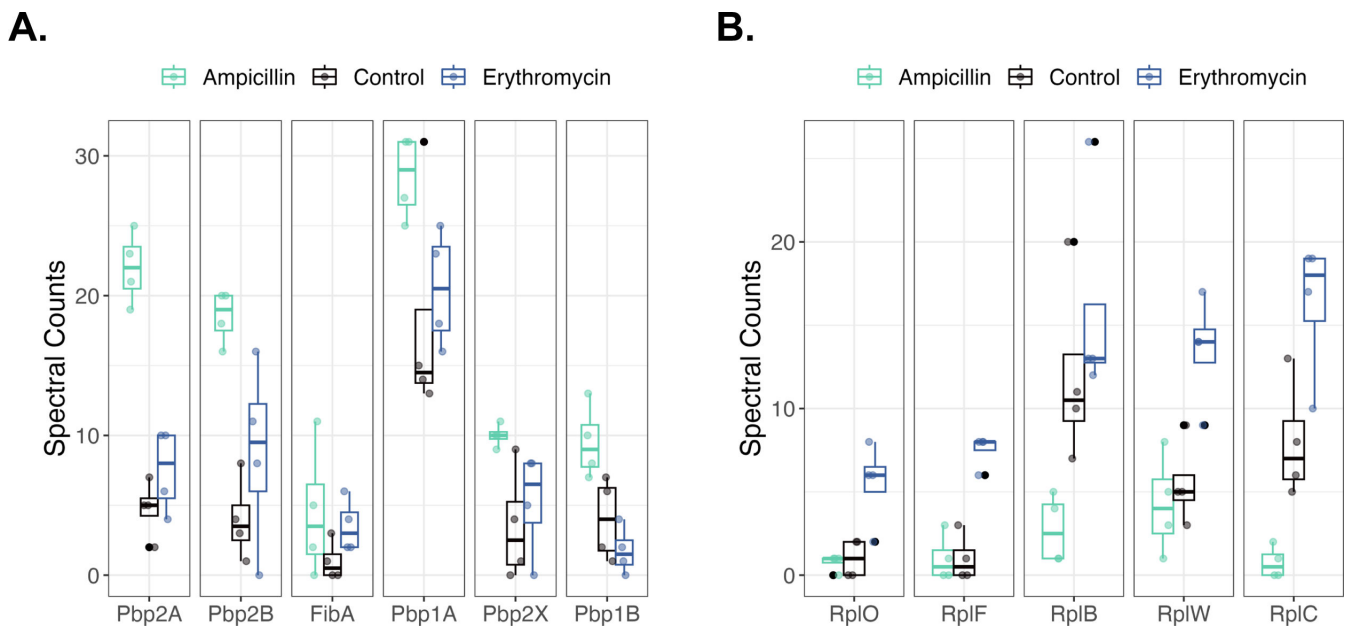


FIG 7 Quantity of proteins identified in MVs from cells treated with ampicillin (turquoise) or erythromycin (blue) or no treatment (control; black). Boxplots represent the summary of spectral counts (y-axis) across biological replicates ($n = 4$) by treatment group for proteins of interest (x-axis). Pairwise Kruskal-Wallis tests of mean spectral counts identified significant differences in MV protein abundances across treatment groups at either P -values < 0.05 or < 0.01 for the (A) penicillin-binding proteins (Pbps) and β -lactam resistance factor (FibA) and the (B) 50S ribosomal proteins.

Ampicillin elicits antimicrobial activity by thinning and destroying the peptidoglycan cell wall, which may explain the increased number of MVs detected in the ampicillin-treated group. Treatment of *S. aureus* with ampicillin was also shown to result in a dose-dependent increase in MV secretion in a prior study (29). Consistent with this explanation, thin-section TEM showed distressed cell walls among the ampicillin-treated GBS as well as the presence of completely lysed cells or non-viable “ghost cells.” A previous study of *Bacillus subtilis* documented a similar increase in MV production following damage to the peptidoglycan by an endolysin along with the detection of ghost cells (42). Nonetheless, assessing cell viability with TEM has limitations, and hence, more imaging studies and use of superior techniques, such as fluorescent dye staining are needed to confirm viability (43) and estimate MV production solely from this cell population. It was suggested that MV production is also a product of cell death with different routes of formation in growing vs dying cells (24, 42). Although MVs secreted from dying cells can still have functional effects, these effects may vary depending on the stressor. In our assessment, more empty or partially empty cells were observed in the ampicillin-treated GBS (Fig. 4; Fig. S3). It is possible that these distinct cell populations could contribute to the functional differences observed in the proteomics analysis; however, additional studies are needed to confirm this observation.

Ampicillin treatment also impacted several cell-wall proteins including MltG and LytR-cpsA-psr (LCP), which were enriched in the MVs from ampicillin-treated GBS compared to MVs from the untreated and erythromycin-treated cells, respectively. MltG, an endolytic murein transglycosylase important for cell wall remodeling and peptidoglycan metabolism, was shown to mediate antibiotic resistance and virulence in *Streptococcus mutans* (44). Similarly, the LCP family proteins are important for cell division, particularly cell envelope maintenance. When depleted, these proteins contributed to decreased cell wall integrity and increased susceptibility of GBS to β -lactam antibiotics (45). Similar investigations in other species provide evidence linking cell-wall weakening and MV release with β -lactam exposure (24, 46). Altogether, these findings indicate that ampicillin treatment of GBS induces the release of MVs due to disruptions in the cell wall.

Future studies, however, are needed to determine the mechanism and clarify whether ampicillin increases the formation of MVs, induces the release of more MVs, or both.

Since erythromycin is not a cell-wall targeting antibiotic, the observed increase in MV production in the erythromycin-treated cells relative to the untreated cells is less clear. Evidence of cell lysis was observed in the thin-section TEMs of the erythromycin-treated GBS as well as the identification of ghost cells, which may partly explain the increase. Another possible explanation could be due to incomplete or stalled growth at cell division septa because of the bacteriostatic effect of this antibiotic. Indeed, the unique cell wall pattern observed in the thin-section TEM of the erythromycin-treated GBS suggests abnormal cell division (39). Additional support for this suggestion comes from a study of MVs in *Salmonella* that were released from cell division septa; these MVs were larger in size containing different proteins compared to MVs released along the cell body (47). Intriguingly, we identified several cell division proteins in the MVs from all three treatment groups, some of which were highly abundant in the MVs from both the ampicillin- and erythromycin-treated GBS. Larger particles were also seen along the streptococcal chains in the SEM images of erythromycin-treated GBS (Fig. S1), which could be indicative of MV release from cell division septa. Nonetheless, more comprehensive microscopy analyses are needed to confirm this finding across samples exposed at different timepoints and growth phases.

Another notable finding was the detection of stress-related proteins in the MVs produced by the antibiotic-treated GBS, which could play a role in how the bacterium responds to antibiotic stress. To survive in stressful conditions, GBS activates the stringent response, which is designed to slow growth and limit non-essential processes (48). MV production has been linked to stress responses in other species (49), and therefore, it is not surprising that we identified several stress-associated proteins to be enriched in the MVs from antibiotic-treated GBS. To facilitate a stringent response, it is plausible that MVs play a role in expelling non-essential factors such as virulence-associated proteins from the bacterial cell. Both CAMP factor and hyaluronate lyase, for example, were enriched or detected exclusively in the MVs from antibiotic-treated GBS relative to the untreated GBS herein. While antibiotic stress may trigger the export of non-essential components to facilitate entry to a dormant survival state, the release of these factors could also enhance cytotoxicity to host cells. Cytotoxic effects by MVs have been observed in GBS and other bacterial species previously (19, 50); hence, these factors may inadvertently impact virulence while promoting bacterial survival.

Prior studies have also shown that MVs mediate resistance to antibiotics by acting as decoys carrying antibiotic targets away from the bacterial cell (24, 51). Based on our detection of ampicillin- and erythromycin-targeting molecules in MVs produced by antibiotic-treated GBS, it is likely that GBS MVs also offer protection from antibiotic-mediated killing. Six PBPs, which are known targets of β -lactam antibiotics like ampicillin, were identified in the MVs from the ampicillin-treated cells; five of these six PBPs were most abundant in these MVs relative to the MVs from the control and erythromycin-treated cells. Similarly, 21 different 50S ribosomal proteins, known targets of erythromycin, were detected in the GBS MVs. Two of these proteins were exclusive to the MVs from erythromycin-treated GBS, and five shared proteins were most abundant in MVs from the erythromycin-treated cultures. While studies in *S. aureus* have shown that MVs can promote antibiotic resistance by transferring resistance to neighboring bacteria (52) or carrying substances (e.g., β -lactamases) that degrade extracellular antibiotics (29), we only detected one resistance determinant, FibA, in the GBS MVs. In *Streptococcus pneumoniae*, *fibA* was shown to be necessary for peptidoglycan crosslinking and resistance to β -lactam antibiotics (53). Altogether, our findings suggest that exposure to ampicillin and erythromycin results in the production of GBS MVs that can serve as decoys carrying antibiotic-specific protein targets outside the bacterial cell. These decoys contribute to the evasion of antibiotic-mediated killing by providing disassociated protein targets to bind to the antibiotic instead of the bacterial cell. In turn, this

extracellular binding can result in a reduction in the overall concentration of antibiotic available as was shown for *S. aureus* (52).

As in all studies, our work has limitations worth noting. First, the use of a single ST-17 cps III GBS strain (GB00112) limits the generalizability of our findings. This strain was isolated from a rectovaginal swab culture collected at a 6 week postpartum visit from an individual who had previously received IAP for prenatal colonization (7) with a strain of the same ST and cps type (15). A genomic comparison of 1,368 GBS core genes detected one silent mutation, or single-nucleotide polymorphism, in the postpartum GB00112 strain relative to the respective prenatal strain despite IAP; both strains had identical virulence and resistance gene profiles (54). We also previously showed that GB00112 can escape antibiotic-mediated killing and produces MVs in the absence of antibiotics with a greater abundance of virulence factors compared to other GBS strains (14, 20). Although the data described herein could partially explain GBS persistence following IAP, future studies are needed to determine if additional strains from persistently colonized patients yield similar results. Another limitation worth noting is that we examined GBS MVs *in vitro* after a 4 h exposure to very high antibiotic concentrations, which may have overestimated the effects relative to those that occur *in vivo* during pregnancy and IAP. Current IAP guidelines for GBS-positive patients recommend administering antibiotics intravenously for a minimum of 4 h to reach adequate antibiotic levels in the amniotic fluid, cord, and neonatal blood (3). In many patients, however, it is not feasible to complete the 4 h treatment due to variable laboring and delivery times. Such variation in antibiotic administration can impact the concentration of GBS in the vaginal tract, thereby making it a difficult system to mimic *in vitro*. Future experiments should, therefore, examine MV production and composition in response to a range of antibiotic doses and treatment durations using a variety of model systems.

Since this is the first study to examine GBS MVs following antibiotic exposure, it serves as a starting point for investigating these MVs in a clinical context. Indeed, our findings have enhanced understanding of how GBS behaves in the presence of two antibiotics commonly used for IAP. While antibiotic treatment contributed to enhanced MV production, only a slight difference in the size of MVs produced by antibiotic-treated and untreated cells was observed. Regardless, it is worth noting that smaller MVs may not have been captured because of the qEV1 size exclusion columns (<35 nm) used in our study, causing us to underestimate the MV size range. Consistent with our findings (Fig. 3A), our prior experiments recovered no GBS MVs < 40 nm during basal growth without antibiotics, while another study of *S. aureus* MVs extracted without size exclusion columns observed no difference in MV size among antibiotic-treated and untreated cells (29). Antibiotic treatment also induced delivery of MVs carrying important proteins that promote bacterial survival in the presence of antibiotics. While some proteins were unique to MVs exposed to both antibiotics, others varied in abundance across treatments. Hence, these findings demonstrate that the production and composition of GBS MVs are dependent on the antibiotic class and highlight how GBS MVs are responsive to and reflective of surrounding environmental factors and stressors.

Importantly, our study uncovered numerous antibiotic targets within MVs from the antibiotic-treated GBS cultures. Many of these targets reveal a mechanism for GBS escape of antibiotic-mediated killing that could promote persistent colonization of the vaginal tract following IAP. Since both antibiotic resistance and persistent GBS colonization threaten the effectiveness of current GBS treatment and prevention methods (6, 7), additional MV studies are necessary. Quantifying MVs from clinical strains of varying genetic backgrounds following antibiotic exposure and exploring their impact on growth and antibiotic tolerance *in vitro* as well as colonization *in vivo* is critical to define their role in evasion and persistence.

ACKNOWLEDGMENTS

We thank Soo H. Ahn and Geoffrey Grzesiak for technical assistance as well as Alicia Withrow, Carol Flegler, and Douglas Whitten for their assistance with microscopy and

proteomics. We would also like to thank Drs. Kathryn Patras and Laura Cook for providing feedback on a prior version of this manuscript.

Financial support was provided by the National Institutes of Health (NIH; AI154192 to S.D.M. and M.G.P.), the Michigan State University (MSU) Research Foundation (to S.D.M.) and, in part, by the Michigan Sequencing and Academic Partnerships for Public Health Innovation and Response (MI-SAPPHIRE) initiative at the MDHHS via CDC through the Epidemiology and Laboratory Capacity for Prevention and Control of Emerging Infectious Diseases Enhancing Detection Expansion program (6NU50CK000510-02-07; to S.D.M.). Salary support was provided by the National Institutes of Health (R01HD090061 to J.A.G. and S.D.M.) and the U.S. Department of Agriculture (2019-67017-29112) to S.D.M. Student support was provided to M.E.P. by the MSU Department of Microbiology, Genetics, and Immunology via the Philipp and Vera Gerhardt Travel and Ralph Evans Awards as well as the MSU College of Natural Science.

Conceptualization: M.E.P., S.D.M.; methodology: M.E.P., C.R.M.; validation and formal analysis: M.E.P., C.R.M.; resources: S.D.M., M.G.P.; supervision and insight: S.D.M., M.G.P., J.A.G.; data curation: M.E.P., S.D.M.; writing—original draft preparation, M.E.P.; writing—review and editing and data visualization: all authors; funding acquisition: S.D.M., M.G.P., J.A.G. All authors have read and agreed to the final version of the manuscript.

AUTHOR AFFILIATIONS

¹Department of Microbiology, Genetics, and Immunology, Michigan State University, East Lansing, Michigan, USA

²Department of Pathology, Microbiology and Immunology, Vanderbilt University Medical Center, Nashville, Tennessee, USA

³Department of Medicine, Vanderbilt University School of Medicine, Nashville, Tennessee, USA

⁴Department of Veterans Affairs, Tennessee Valley Healthcare Systems, Nashville, Tennessee, USA

⁵Division of Infectious Diseases, Department of Medicine, Indiana University School of Medicine, Indianapolis, Indiana, USA

⁶Department of Pathobiology and Diagnostic Investigation, Michigan State University, East Lansing, Michigan, USA

PRESENT ADDRESS

Cole R. McCutcheon, Department of Integrative Immunobiology, Duke University Medical Center, Durham, North Carolina, USA

AUTHOR ORCIDs

Macy E. Pell  <http://orcid.org/0000-0002-1846-5063>

Jennifer A. Gaddy  <http://orcid.org/0000-0002-2192-4224>

Shannon D. Manning  <http://orcid.org/0000-0001-9581-0660>

FUNDING

| Funder | Grant(s) | Author(s) |
|--|---------------------|---|
| National Institutes of Health | AI154192 | Margaret G. Petroff Shannon D. Manning |
| AgBioResearch, Michigan State University | | Shannon D. Manning |
| Michigan State University Research Foundation | | Shannon D. Manning |
| Michigan Department of Health and Human Services | 6NU50CK000510-02-07 | Shannon D. Manning |

| Funder | Grant(s) | Author(s) |
|--|------------------|--------------------------------------|
| U.S. Department of Agriculture | 2019-67017-29112 | Shannon D. Manning |
| National Institutes of Health | HD090061 | Jennifer Gaddy Shannon D. Manning |
| Michigan State University College of Natural Science | | Macy E. Pell |

AUTHOR CONTRIBUTIONS

Macy E. Pell, Conceptualization, Data curation, Formal analysis, Investigation, Methodology, Validation, Visualization, Writing – original draft, Writing – review and editing | Cole R. McCutcheon, Formal analysis, Investigation, Methodology, Writing – review and editing | Jennifer A. Gaddy, Funding acquisition, Investigation, Writing – review and editing | David M. Aronoff, Writing – review and editing | Margaret G. Petroff, Funding acquisition, Investigation, Resources, Writing – review and editing | Shannon D. Manning, Conceptualization, Funding acquisition, Investigation, Project administration, Resources, Supervision, Validation, Visualization, Writing – review and editing

DATA AVAILABILITY

Data sets are available in the supplementary tables. Raw proteomic data were submitted to the MassIVE database as data set [MSV000094926](https://doi.org/doi:10.25345/CSRV0DB88) and can be accessed at <https://doi.org/doi:10.25345/CSRV0DB88>. R scripts used for data analysis and visualization can be found at https://github.com/macyEpell/Pell_GBS_MVs_2024.

ADDITIONAL FILES

The following material is available [online](#).

Supplemental Material

Supplemental figures (Spectrum03223-24-S0001.pdf). Figures S1 to S4.

Supplemental tables (Spectrum03223-24-S0002.xlsx). Tables S1 to S3.

REFERENCES

- Seale AC, Bianchi-Jassir F, Russell NJ, Kohli-Lynch M, Tann CJ, Hall J, Madrid L, Blencowe H, Cousens S, Baker CJ, Bartlett L, Cutland C, Gravett MG, Heath PT, Ip M, Le Doare K, Madhi SA, Rubens CE, Saha SK, Schrag SJ, Sobanjo-Ter Meulen A, Vekemans J, Lawn JE. 2017. Estimates of the burden of group B Streptococcal disease worldwide for pregnant women, stillbirths, and children. *Clin Infect Dis* 65:S200–S219. <https://doi.org/10.1093/cid/cix664>
- Russell NJ, Seale AC, O'Driscoll M, O'Sullivan C, Bianchi-Jassir F, Gonzalez-Guarin J, Lawn JE, Baker CJ, Bartlett L, Cutland C, et al. 2017. Maternal colonization with group B *Streptococcus* and serotype distribution worldwide: systematic review and meta-analyses. *Clin Infect Dis* 65:S100–S111. <https://doi.org/10.1093/cid/cix658>
- American College of Obstetricians and Gynecologists. 2020. Prevention of group B streptococcal early-onset disease in newborns. *Obstetrics & Gynecology* 135:e51–e72. <https://doi.org/10.1097/AGO.00000000000003668>
- Schrag SJ, Verani JR. 2013. Intrapartum antibiotic prophylaxis for the prevention of perinatal group B streptococcal disease: experience in the United States and implications for a potential group B streptococcal vaccine. *Vaccine (Auckl)* 31 Suppl 4:D20–6. <https://doi.org/10.1016/j.vaccine.2012.11.056>
- Le Doare K, O'Driscoll M, Turner K, Seedat F, Russell NJ, Seale AC, Heath PT, Lawn JE, Baker CJ, Bartlett L, Cutland C, Gravett MG, Ip M, Madhi SA, Rubens CE, Saha SK, Schrag S, Sobanjo-Ter Meulen A, Vekemans J, Kampmann B, GBS Intrapartum Antibiotic Investigator Group. 2017. Intrapartum antibiotic chemoprophylaxis policies for the prevention of group B streptococcal disease Worldwide: systematic review. *Clin Infect Dis* 65:S143–S151. <https://doi.org/10.1093/cid/cix654>
- Nanduri SA, Petit S, Smelser C, Apostol M, Alden NB, Harrison LH, Lynfield R, Vagnone PS, Burzlaff K, Spina NL, Dufort EM, Schaffner W, Thomas AR, Farley MM, Jain JH, Pondo T, McGee L, Beall BW, Schrag SJ. 2019. Epidemiology of invasive early-onset and late-onset group B streptococcal disease in the United States, 2006 to 2015. *JAMA Pediatr* 173:224. <https://doi.org/10.1001/jamapediatrics.2018.4826>
- Spaetgens R, DeBella K, Ma D, Robertson S, Mucenski M, Davies HD. 2002. Perinatal antibiotic usage and changes in colonization and resistance rates of group B *Streptococcus* and other pathogens. *Obstet Gynecol* 100:525–533. [https://doi.org/10.1016/s0029-7844\(02\)02068-9](https://doi.org/10.1016/s0029-7844(02)02068-9)
- Rubens CE, Wessels MR, Heggen LM, Kasper DL. 1987. Transposon mutagenesis of type III group B *Streptococcus*: correlation of capsule expression with virulence. *Proc Natl Acad Sci USA* 84:7208–7212. <https://doi.org/10.1073/pnas.84.20.7208>
- Madrid L, Seale AC, Kohli-Lynch M, Edmond KM, Lawn JE, Heath PT, Madhi SA, Baker CJ, Bartlett L, Cutland C, Gravett MG, Ip M, Le Doare K, Rubens CE, Saha SK, Sobanjo-Ter Meulen A, Vekemans J, Schrag S, Infant GBS Disease Investigator Group. 2017. Infant group B streptococcal disease incidence and serotypes worldwide: Systematic review and meta-analyses. *Clin Infect Dis* 65:S160–S172. <https://doi.org/10.1093/cid/cix656>
- Jones N, Oliver KA, Barry J, Harding RM, Bisharat N, Spratt BG, Peto T, Crook DW, Oxford Group B *Streptococcus* Consortium. 2006. Enhanced invasiveness of bovine-derived neonatal sequence type 17 group B *Streptococcus* is independent of capsular serotype. *Clin Infect Dis* 42:915–924. <https://doi.org/10.1086/500324>
- Manning SD, Springman AC, Lehotzky E, Lewis MA, Whittam TS, Davies HD. 2009. Multilocus sequence types associated with neonatal group B

- streptococcal sepsis and meningitis in Canada. *J Clin Microbiol* 47:1143–1148. <https://doi.org/10.1128/JCM.01424-08>
12. Jones N, Bohnsack JF, Takahashi S, Oliver KA, Chan M-S, Kunst F, Glaser P, Rusniok C, Crook DWM, Harding RM, Bisharat N, Spratt BG. 2003. Multilocus sequence typing system for group B *Streptococcus*. *J Clin Microbiol* 41:2530–2536. <https://doi.org/10.1128/JCM.41.6.2530-2536.2003>
 13. Korir ML, Knupp D, LeMerise K, Boldenow E, Loch-Carusio R, Aronoff DM, Manning SD. 2014. Association and virulence gene expression vary among serotype III group B *Streptococcus* isolates following exposure to decidual and lung epithelial cells. *Infect Immun* 82:4587–4595. <https://doi.org/10.1128/IAI.02181-14>
 14. Korir ML, Laut C, Rogers LM, Plemmons JA, Aronoff DM, Manning SD. 2017. Differing mechanisms of surviving phagosomal stress among group B *Streptococcus* strains of varying genotypes. *Virulence* 8:924–937. <https://doi.org/10.1080/21505594.2016.1252016>
 15. Manning SD, Lewis MA, Springman AC, Lehotzky E, Whittam TS, Davies HD. 2008. Genotypic diversity and serotype distribution of group B *Streptococcus* isolated from women before and after delivery. *Clin Infect Dis* 46:1829–1837. <https://doi.org/10.1093/cid/ciz033>
 16. Tazi A, Plainvert C, Anselem O, Ballon M, Marcou V, Seco A, El Alaoui F, Joubrel C, El Helali N, Falloukh E, Frigo A, Raymond J, Trieu-Cuot P, Branger C, Le Monnier A, Azria E, Ancel PY, Jarreau PH, Mandelbrot L, Goffinet F, Poyart C. 2019. Risk factors for infant colonization by hypervirulent CC17 Group B *Streptococcus*: toward the understanding of late-onset disease. *Clin Infect Dis* 69:1740–1748. <https://doi.org/10.1093/cid/ciz033>
 17. Schwechheimer C, Kuehn MJ. 2015. Outer-membrane vesicles from Gram-negative bacteria: biogenesis and functions. *Nat Rev Microbiol* 13:605–619. <https://doi.org/10.1038/nrmicro3525>
 18. Brown L, Wolf JM, Prados-Rosales R, Casadevall A. 2015. Through the wall: extracellular vesicles in Gram-positive bacteria, mycobacteria and fungi. *Nat Rev Microbiol* 13:620–630. <https://doi.org/10.1038/nrmicro3480>
 19. Surve MV, Anil A, Kamath KG, Bhutda S, Sthanam LK, Pradhan A, Srivastava R, Basu B, Dutta S, Sen S, Modi D, Banerjee A. 2016. Membrane vesicles of group B *Streptococcus* disrupt feto-maternal barrier leading to preterm birth. *PLoS Pathog* 12:e1005816. <https://doi.org/10.1371/journal.ppat.1005816>
 20. McCutcheon CR, Pell ME, Gaddy JA, Aronoff DM, Petroff MG, Manning SD. 2021. Production and composition of group b streptococcal membrane vesicles vary across diverse lineages. *Front Microbiol* 12:770499. <https://doi.org/10.3389/fmicb.2021.770499>
 21. Armistead B, Quach P, Snyder JM, Santana-Ufret V, Furuta A, Brokaw A, Rajagopal L. 2021. Hemolytic membrane vesicles of group B *Streptococcus* promote infection. *J Infect Dis* 223:1488–1496. <https://doi.org/10.1093/infdis/jiaa548>
 22. McCutcheon CR, Gaddy JA, Aronoff DM, Manning SD, Petroff MG. 2025. Group B streptococcal membrane vesicles induce proinflammatory cytokine production and are sensed in an nlrp3 inflammasome-dependent mechanism in a human macrophage-like cell line. *ACS Infect Dis* 11:453–462. <https://doi.org/10.1021/acscinfeddis.4c00641>
 23. Kadurugamuwa JL, Beveridge TJ. 1995. Virulence factors are released from *Pseudomonas aeruginosa* in association with membrane vesicles during normal growth and exposure to gentamicin: a novel mechanism of enzyme secretion. *J Bacteriol* 177:3998–4008. <https://doi.org/10.1128/jb.177.14.3998-4008.1995>
 24. Andreoni F, Toyofuku M, Menzi C, Kalawong R, Mairpady Shambat S, François P, Zinkernagel AS, Eberl L. 2019. Antibiotics stimulate formation of vesicles in *Staphylococcus aureus* in both phage-dependent and -independent fashions and via different routes. *Antimicrob Agents Chemother* 63:1–10. <https://doi.org/10.1128/AAC.01439-18>
 25. Bos J, Cisneros LH, Mazel D. 2021. Real-time tracking of bacterial membrane vesicles reveals enhanced membrane traffic upon antibiotic exposure. *Sci Adv* 7:eabd1033. <https://doi.org/10.1126/sciadv.abd1033>
 26. Li Q, Li J, He T, Ji X, Wei R, Yu M, Wang R. 2024. Sub-MIC antibiotics modulate productions of outer membrane vesicles in tigeicycline-resistant *Escherichia coli* Antibiotics (Basel) 13:276. <https://doi.org/10.3390/antibiotics13030276>
 27. Bauwens A, Kunsmann L, Karch H, Mellmann A, Bielaszewska M. 2017. Antibiotic-mediated modulations of outer membrane vesicles in enterohemorrhagic *Escherichia coli* O104:H4 and O157:H7. *Antimicrob Agents Chemother* 61:e00937-17. <https://doi.org/10.1128/AAC.00937-17>
 28. Kim SW, Lee JS, Park SB, Lee AR, Jung JW, Chun JH, Lazarte JMS, Kim J, Seo J-S, Kim J-H, Song J-W, Ha MW, Thompson KD, Lee C-R, Jung M, Jung TS. 2020. The importance of porins and β -lactamase in outer membrane vesicles on the hydrolysis of β -lactam antibiotics. *Int J Mol Sci* 21:2822. <https://doi.org/10.3390/ijms21082822>
 29. Kim SW, Seo J-S, Park SB, Lee AR, Lee JS, Jung JW, Chun JH, Lazarte JMS, Kim J, Kim J-H, Song J-W, Franco C, Zhang W, Ha MW, Paek S-M, Jung M, Jung TS. 2020. Significant increase in the secretion of extracellular vesicles and antibiotics resistance from methicillin-resistant *Staphylococcus aureus* induced by ampicillin stress. *Sci Rep* 10:1–14. <https://doi.org/10.1038/s41598-020-78121-8>
 30. Schooling SR, Beveridge TJ. 2006. Membrane vesicles: an overlooked component of the matrices of biofilms. *J Bacteriol* 188:5945–5957. <https://doi.org/10.1128/JB.00257-06>
 31. Singh P, Springman AC, Davies HD, Manning SD. 2012. Whole-genome shotgun sequencing of a clonizing multilocus sequence type 17 *Streptococcus agalactiae* strain. *J Bacteriol* 194:6005–6005. <https://doi.org/10.1128/JB.01378-12>
 32. Nguyen SL, Greenberg JW, Wang H, Collaer BW, Wang J, Petroff MG. 2019. Quantifying murine placental extracellular vesicles across gestation and in preterm birth data with tidyNano: a computational framework for analyzing and visualizing nanoparticle data in R. *PLoS One* 14:e0218270. <https://doi.org/10.1371/journal.pone.0218270>
 33. Perkins DN, Pappin DJC, Creasy DM, Cottrell JS. 1999. Probability-based protein identification by searching sequence databases using mass spectrometry data. *Electrophoresis* 20:3551–3567. [https://doi.org/10.1002/\(SICI\)1522-2683\(19991201\)20:18<3551::AID-ELPS3551>3.0.CO;2-2](https://doi.org/10.1002/(SICI)1522-2683(19991201)20:18<3551::AID-ELPS3551>3.0.CO;2-2)
 34. Wickham H, Averick M, Bryan J, Chang W, McGowan L, François R, Grolemund G, Hayes A, Henry L, Hester J, Kuhn M, Pedersen T, Miller E, Bache S, Müller K, Ooms J, Robinson D, Seidel D, Spinu V, Takahashi K, Vaughan D, Wilke C, Woo K, Yutani H. 2019. Welcome to the Tidyverse. *JOS* 4:1686. <https://doi.org/10.21105/joss.01686>
 35. Hadley W. 2009. Ggplot2: elegant graphics for data analysis. *Journal of Statistical Software*. Available from: <https://www.jstatsoft.org/article/view/v035b01/406>
 36. Chen H, Boutros PC. 2011. VennDiagram: a package for the generation of highly-customizable venn and euler diagrams in R. *BMC Bioinformatics* 12:35. <https://doi.org/10.1186/1471-2105-12-35>
 37. Kassambara A. 2023. Rstatix: pipe-friendly framework for basic statistical tests. R package version 0.7.2. <https://cran.r-project.org/web/packages/rstatix/index.html>
 38. Lorian V, Fernandes F. 1999. Electron microscopy studies of the bactericidal effects of quinupristin/dalfopristin on *Staphylococcus aureus*. *J Antimicrob Chemother* 43:845. <https://doi.org/10.1093/jac/43.6.845>
 39. Kawai M, Yamagishi J. 2009. Mechanisms of action of acriflavine: electron microscopic study of cell wall changes induced in *Staphylococcus aureus* by acriflavine. *Microbiol Immunol* 53:481–486. <https://doi.org/10.1111/j.1348-0421.2009.00151.x>
 40. Toyofuku M, Nomura N, Eberl L. 2019. Types and origins of bacterial membrane vesicles. *Nat Rev Microbiol* 17:13–24. <https://doi.org/10.1038/s41579-018-0112-2>
 41. Briaud P, Carroll RK. 2020. Extracellular vesicle biogenesis and functions in gram-positive bacteria. *Infect Immun* 88:1–14. <https://doi.org/10.1128/IAI.00433-20>
 42. Toyofuku M, Cárcamo-Oyarce G, Yamamoto T, Eisenstein F, Hsiao CC, Kurosawa M, Gademann K, Pilhofer M, Nomura N, Eberl L. 2017. Phage-triggered membrane vesicle formation through peptidoglycan damage in *Bacillus subtilis*. *Nat Commun* 8:481. <https://doi.org/10.1038/s41467-017-00492-w>
 43. Johnson MB, Criss AK. 2013. Fluorescence microscopy methods for determining the viability of bacteria in association with mammalian cells. *JoVE*, no. 79:50729. <https://doi.org/10.3791/50729-v>
 44. Zaidi S, Ali K, Chawla YM, Khan AU. 2023. mltG gene deletion mitigated virulence potential of *Streptococcus mutans*: An *in-vitro*, *ex-situ* and *in-vivo* study. *AMB Express* 13:19. <https://doi.org/10.1186/s13568-023-01526-x>
 45. Rajaei A, Rowe HM, Neely MN. 2022. The LCP family protein, Psr, is required for cell wall integrity and virulence in *Streptococcus agalactiae* Microorganisms 10:217. <https://doi.org/10.3390/microorganisms10020217>
 46. Biagini M, Garibaldi M, Aprea S, Pezzicoli A, Doro F, Becherelli M, Taddei AR, Tani C, Tavarini S, Mora M, Teti G, D'Oro U, Nuti S, Soriani M, Margarit I, Rappuoli R, Grandi G, Norais N. 2015. The human pathogen

- Streptococcus pyogenes* releases lipoproteins as lipoprotein-rich membrane vesicles. *Mol Cell Proteomics* 14:2138–2149. <https://doi.org/10.1074/mcp.M114.045880>
47. Deatherage BL, Lara JC, Bergsbaken T, Rassoulian Barrett SL, Lara S, Cookson BT. 2009. Biogenesis of bacterial membrane vesicles. *Mol Microbiol* 72:1395–1407. <https://doi.org/10.1111/j.1365-2958.2009.06731.x>
 48. Hooven TA, Catomeris AJ, Bonakdar M, Tallon LJ, Santana-Cruz I, Ott S, Daugherty SC, Tettelin H, Ratner AJ. 2018. The *Streptococcus agalactiae* stringent response enhances virulence and persistence in human blood. *Infect Immun* 86:1–15. <https://doi.org/10.1128/IAI.00612-17>
 49. Mozaheb N, Mingeot-Leclercq MP. 2020. Membrane Vesicle production as a bacterial defense against stress. *Front Microbiol* 11:600221. <https://doi.org/10.3389/fmicb.2020.600221>
 50. Wang X, Koffi PF, English OF, Lee JC. 2021. *Staphylococcus aureus* extracellular vesicles: a story of toxicity and the stress of 2020. *Toxins* 13:75. <https://doi.org/10.3390/toxins13020075>
 51. Park J, Kim M, Shin B, Kang M, Yang J, Lee TK, Park W. 2021. A novel decoy strategy for polymyxin resistance in *Acinetobacter baumannii* Elife 10:1–29. <https://doi.org/10.7554/eLife.66988>
 52. Lee AR, Park SB, Kim SW, Jung JW, Chun JH, Kim J, Kim YR, Lazarte JMS, Jang HB, Thompson KD, Jung M, Ha MW, Jung TS. 2022. Membrane vesicles from antibiotic-resistant *Staphylococcus aureus* transfer antibiotic-resistance to antibiotic-susceptible *Escherichia coli*. *J Appl Microbiol* 132:2746–2759. <https://doi.org/10.1111/jam.15449>
 53. Weber B, Ehlert K, Diehl A, Reichmann P, Labischinski H, Hakenbeck R. 2000. The fib locus in *Streptococcus pneumoniae* is required for peptidoglycan crosslinking and PBP-mediated beta-lactam resistance. *FEMS Microbiol Lett* 188:81–85. <https://doi.org/10.1111/j.1574-6968.2000.tb09172.x>
 54. Pell ME, Blankenship HM, Gaddy JA, Davies HD, Manning SD. 2024. Intrapartum antibiotic prophylaxis selects for mutators in group B streptococci among persistently colonized patients. *bioRxiv*:2024.04.01.587590. <https://doi.org/10.1101/2024.04.01.587590>